RSC Advances

ROYAL SOCIETY OF CHEMISTRY

www.rsc.org/advances

Immobilization of Acetylcholinesterase on Electrospun Poly (acrylic acid)/Multi-walled Carbon Nanotubes Nanofibrous Membranes

Seyed Vahid Ebadi[1], Aref Fakhrali[1], Seyed Omid Ranaei-Siadat[2], Ali Akbar Gharehaghaji[1*], Saeedeh Mazinani[3*], Mohammad Dinari[4], Javad Harati[2]

[1] Department of Textile Engineering, Amirkabir University of Technology, 424 Hafez Ave, 15875-4413 Tehran, Iran.

[2] Nano-Biotechnology Engineering Lab., Department of Biotechnology, Faculty of Energy Engineering and New Technologies, Shahid Beheshti University, GC, Tehran, Iran.

[3] Amirkabir Nanotechnology Research Institute (ANTRI), Amirkabir University of Technology (Polytechnic of Tehran), 424 Hafez Ave, 15875-4413 Tehran, Iran.

[4] Organic Polymer Chemistry Research Laboratory, Department of Chemistry, Isfahan University of Technology, Isfahan, 84156-83111, Isfahan, Iran.

Abstract

[*] Corresponding Authors:

Ali Akbar Gharehaghaji; aghaji@aut.ac.ir

Department of Textile Engineering, Amirkabir University of Technology,424 Hafez Ave, 15875-4413 Tehran, Iran. Tel & Fax No. +98 21 64542616.

Saeedeh Mazinani; s.mazinani@aut.ac.ir

Amirkabir Nanotechnology Research Institute (ANTRI), Amirkabir University of Technology (Polytechnic of Tehran), 424 Hafez Ave, 15875-4413 Tehran, Iran. Tel & Fax No. (+98) 21-66402441.

In this work, poly (acrylic acid) (PAA) and PAA/multi-walled carbon nanotubes (MWNTs) nanofibrous membranes are fabricated by electrospinning to immobilize acetylcholinesterase (AChE). 3-Aminopropyltriethoxysilane (APTES) and glutaraldehyde are used for surface modification and PAA membrane stabilization in aqueous media. The structure of the nanofibrous membrane was studied by scanning electron microscopy (SEM), Fourier transform infrared spectroscopy, thermogravimetric and mechanical analyses. The AChE enzyme was immobilized on PAA nanofibers with different amounts of MWNTs concentrations from 0 to 5 wt%. The SEM images revealed that the average diameter of PAA nanofibers was 226±25 nm which was increased by increasing the MWNTs concentration. The tensile strength and modulus of nanofibrous membranes increased 1.87 and 4.39 fold respectively after crosslinking process. The results show that membranes containing MWNTs are more appropriate support for enzyme immobilization. In comparison to pure PAA, the activity of the sample containing 4 wt% of MWNTs was increased 5.07 fold. Also, the immobilized enzyme showed excellent reusability even after 10 cycles of washing and samples maintained more than 90% of their original activities. Moreover, pH and thermal stability of immobilized enzyme was improved compared to free enzyme. The results show that PAA/MWNTs nanofibrous membrane could be accounted as a suitable support for AChE immobilization in addition to different applications such as biosensor manufacturing.

Keywords: Electrospinning; Poly (acrylic acid) nanofibers; Enzyme immobilization; Acetylcholinesterase; Carbon nanotubes.

1. Introduction

Enzymes are beneficial proteins which catalyze chemical reactions with reducing the activation energy of reaction.[1] The unique properties of enzymes make them useful for many applications such as biosensors, pharmaceuticals, food processing, biofuel cell production and etc.[2-6] However, these industrial applications are limited and expensive due to the instability and difficult recovery and non-reusability of enzymes. Immobilization of enzymes on a solid support is a popular strategy to overcome these limitations.[7, 8] Moreover, immobilization process may improve other enzyme properties such as observed activity, specificity and selectivity, etc.[9] Also, the enzyme immobilization may be used in reduction of enzyme inhibition caused by high concentrations of the substrate or by some reaction products that is a problem in some reactions and decreases the enzyme activity.[10] The generation of favorable environments surrounding the enzymes has been reported as a strategy for prevention of enzyme inactivation against some of inactivation agents (e.g., organic solvents, oxygen, hydrogen peroxide and dissolved gases). In this case, enzyme immobilization on designed supports can be used effectively to produce hydrophobic or hydrophilic environments around the enzymes. [11]

There are many researches focused on the enzyme immobilization techniques to convert it into a powerful tool to improve enzyme performances.[12-14] An intense multipoint covalent immobilization of enzymes on a proper support can increase enzyme rigidity and therefore improves the stability of the enzyme against any inactivating agent that produces conformational changes.[10, 15] Prevention of subunit dissociation of multimeric enzymes is one of the most interesting goals of enzyme immobilization. In multimerc enzymes that formed by different subunits, dissociation of subunits is the main reason for inactivation of these enzymes.[12] Thus, to prevent this phenomenon, one bond between each subunit and support should be enough. Nevertheless, a further multipoint covalent attachment of each enzyme subunit can result in more

effective stabilization of multimeric enzymes.[15] For this goal, using a proper support and suitable immobilization conditions (e.g., reaction time, pH value, temperature, buffers, etc.) is necessary to achieve an effective multipoint or multisubunit immobilization.[9, 15] In this case, a simple adsorption of the enzyme on an ion exchanger support may be enough.[15] It should be noted that subunit immobilization becomes more difficult when increases the complexity of the enzyme. Thus, dimeric enzymes may be easily stabilized on activated supports via adsorption or covalent attachment.[11]

Glutaraldehyde is a known crosslinker agent that has been used in many applications such as activation of supports, crosslinking of proteins, and crosslinking of enzymes and supports. The use of glutaraldehyde technique for the enzyme immobilization is very versatile and is used successfully for the immobilization of various enzymes on the different supports. In fact, the glutaraldehyde activated supports could be considered as heterofunctional supports. Depending on the experimental conditions, the activated supports with glutaraldehyde may give three types of interactions (covalent, ionic exchange and hydrophobic adsorption) with an enzyme which leads to the good crosslinking process.[16, 17]

In recent few years, different nanostructured materials such as mesoporous silica, nanotubes, nanoparticles, and nanofibers were widely used as a support for enzyme immobilization.[18-20] High specific surface area and porous structure of electrospun nanofibers provide higher enzyme loading to make them useful for enzyme immobilization. In addition, the surface of nanofibers can be modified to more effective immobilization. Also, in contrast to nanoparticles, nanofiber supports can be easily recovered and reused. Hence, immobilization of enzymes on various polymeric nanofibers has been widely reported by different researchers.[21-23]

Another nanostructured material which has been widely used recently for immobilization of enzymes are carbon nanotubes (CNTs).[24] The unique properties of carbon nanotubes such as mechanical [25], electrical [26] and thermal properties [27], as well as biocompatibility [24] has made them proper candidates for many applications. Electrospinning is a useful technique to produce polymer/CNTs nanocomposites including CNTs orienting parallel to the nanofibers main axis.[28-30] Utilizing CNTs in polymeric nanofibers increases the mechanical stability of nanofibers under operating conditions along the fiber axis.[31]

Acetylcholine (ACh) is the main neurotransmitter in cholinergic system and acetylcholinesterase (AChE) (E.C 3.1.1.7) is a serine hydrolase, which catalyzes the hydrolysis of neurotransmitter acetylcholine into choline and acetate. An inhibitor of AChE enzyme is carbamates and organophosphates, which presents in agricultural pesticides and chemical warfare agents (nerve agents). The inhibition of this enzyme accumulates ACh in the synaptic gap and blocks the nerve signal transfer into the postsynaptic membrane. Hence, the detection of AChE inhibitors (insecticide residues) with the important goal of ensuring human, animal and environmental safety is essential. These inhibitors can be detected by using biosensors which are using AChE as biological element. Preparation of an effective biosensor requires a suitable immobilization of enzyme in a stable and active condition besides reusability.[32, 33] Acetylcholinesterase from *Drosophila* is a dimeric enzyme that each subunit of it is composed of two noncovalently linked polypeptides of 18 and 55 kDa which arise from the processing of a 75-kDa precursor. Also, *Drosophila* AChE has four sites of Asn-linked Glycosylation.[34] Thus, AChE has been characterized as a dimeric enzyme composed of two active subunits that are associated together by a disulfide bond and each is composed of two polypeptides (55 and 18 kDa) which remain noncovalently associated to form the active subunit.[34]

Different nanofibrous membranes were used for AChE immobilization for improvement in enzyme loading as well as thermal and operational stability. [35-37] Also, Amini et al. immobilized AChE on polyacrylamide/MWNTs nanofibers and the results showed that CNT improve the enzyme immobilization.[38]

Poly (acrylic acid) (PAA) is a weak anionic polyelectrolyte and contains carboxylic groups. Hydrogel networks formed from PAA are able to absorb water many times more than their weight to be employed in many applications.[39] The research results of Liu et al. demonstrated that PAA/MWNTs composite can be used to anchor biomacromolecules such as enzymes and DNA, which provides the possibility of developing bioelectronic devices and biosensing applications.[40]

There is not a reported study on the enzyme immobilization on PAA nanofibers in literature and we for the first time use this support to immobilize AChE. In the present study, PAA and PAA/MWNTs nanofibrous membranes are prepared by electrospinning as a support for immobilization of AChE for the first time, besides using 3-aminopropyltriethoxysilane (APTES) as surface modifier and glutaraldehyde as the crosslinking agent. The activity, pH and thermal stability of the immobilized enzyme on different PAA/MWNTs nanofibers membranes are studied. Our results showed excellent reusability for the immobilized enzyme in comparison with other studies for AChE immobilization on nanofibrous membranes.[35-37]

2. Experimental

2.1. Materials

Poly (acrylic acid) (PAA, M_v=450,000), acetylthiocholine iodide (ATChI) and 5,5´-dithio-bis-(2-nitrobenzoic acid) (DTNB) were purchased from Sigma-Aldrich Chemical Co. and

deionized water was used as solvent. 3-Aminopropyltriethoxysilane (APTES) and glutaraldehyde (GA, 25% aqueous solution) were purchased from Merck Chemical Co. Multi-walled carbon nanotubes (MWNTs) with 10-20 nm outer diameter, 20 μm length and 95% purity were used to obtain nanocomposite nanofibers. An ionic surfactant, sodium dodecyl sulphate (SDS, M_W=288.38) was purchased from BDH Chemical Co. *Pichia Pastoris* was purchased from Invitrogen Co. and all other agents used in the experiments were of analytical grade and were obtained from Merck Chemical Co. and used as received.

2.2. Preparation of nanofibrous membranes

PAA aqueous solution (5 w/v%) was prepared by dissolving PAA powder in deionized water by using magnetic stirrer for 8 h at room temperature. For preparing PAA/MWNTs solutions; at first 1 w/v% of SDS was dissolved in water using magnetic stirrer for 1 h, then different weight percentages of MWNTs (0.5, 1, 2, 3, 4 and 5 wt%) were dispersed in water/SDS solutions and then it was sonicated for 45 min. Finally, electrospinning solutions were prepared by dissolving 5 w/v% of PAA in solutions using magnetic stirrer for 8 h at room temperature.

Electrospinning setup was consisted of a high-voltage DC power supply, a syringe pump (KD100, KD Scientific), with a needle tip (22 Gauge, Length=34 mm, Outer diameter = 0.7 mm, Inner diameter = 0.4 mm) and a collector which was grounded and covered with aluminum foil. The distance between the needle tip and collector was set at 20 cm. Moreover, a voltage of 14 kV was applied and the flow rate of polymer solutions was kept at 0.5 mL/h.

2.3. Enzyme production

Gene sequence of *Drosophila melanogaster* acetylcholinesterase enzyme was cloned into the pPinkα-HC vector and then was transformed into *Pichia pastoris* using electroporation method. The enzyme was expressed and secreted into the culture medium during the process. All processes were carried out according to the instruction manual of Invitrogen.

2.4. Crosslinking and enzyme immobilization

For enzyme immobilization, at first, all nanofibrous membranes were prepared at the same size of 1 × 1 cm and samples were immersed in 40 v/v % of APTES solution in methanol for 12 h at room temperature. The resulting samples were placed in 1 v/v % of GA solution in methanol for 4 h at 80 ºC. Subsequently, the samples were well washed several times using distilled water to remove any residual unreacted GA and APTES. Then, the samples were left in AChE solution in 0.1 M sodium phosphate buffer solution (pH 7.0) for 20 h in cold room at 4 ºC under shaking for enzyme immobilization. Finally, the samples were well washed several times using phosphate buffer solution (25 mM, pH 7.4) and the activity of immobilized enzyme was measured.

2.5. Measurements and characterizations

The surface morphology of nanofibers was studied by scanning electron microscopy (SEM) (XL-30, Philips) after coating samples with gold. The average diameter of nanofibers was obtained by measuring the diameters of 100 nanofibers employing ImageJ software (National Institute of Health, USA). Thermogravimetric analysis (TGA) (TG 209 F1, Netzsch) of samples before and after crosslinking and enzyme immobilization was performed under a nitrogen

atmosphere at a heating rate of 10 ºC/min from 30 to 800 ºC. Fourier transform infrared (FTIR) spectra of samples were taken from 4000 to 500 cm^{-1} using a Nexus 670 spectrometer (Nicolet, USA). Mechanical properties of nanofiber layers before and after crosslinking were measured by the tensile tester (Instron, 5566) with a 50 N load-cell at room temperature. The samples were cut into 5 mm width and 30 mm length and the thickness of the samples was measured with a thickness gauge. The sample gauge length was 20 mm and the extension rate of samples was set at 2 mm/min. The reported tensile strength, tensile modulus, and elongation at break represented average results of five tests for each sample.

The activity of the free and immobilized AChE was measured according to Ellman's method [41] using 1 mM ATChI as substrate and DTNB as chromogen. For immobilized enzyme assay, each sample was added to 1 mL reaction mixture and then increasing absorbance was measured at 412 nm via UV-vis spectrophotometer (T80+, PG Instruments) after 1 min. One unit of enzymatic activity defined as the amount of enzyme which catalyzes 1 μmol of substrate to product per minute. All reactions and measurements were carried out at room temperature. Moreover, the kinetic parameters for both immobilized and free enzymes were measured by different ATChI concentrations (ranging from 0.005 to 1.5 mM) as substrate. The activity of free and immobilized enzyme was measured in the range of 5-60 ºC and the pH range of 5.6–10.2 to investigate the effect of temperature and pH changes. The reusability of immobilized AChE was studied by measuring its activity after 10 cycles of reusing. After each measurement, samples were washed out several times with phosphate buffer solution. All experimental points are the average of three independent experiments.

3. Results and discussion

3.1. Morphology of membranes

Figure 1 shows the SEM images of pure nanofibers and PAA/MWNTs nanocomposite nanofibers at different concentrations of nanotubes. As it can be seen, the surface morphology of pure PAA nanofibers is smooth and fine beadless nanofibers were obtained with 5 w/v % of PAA solution. Moreover, the surface of PAA/MWNTs nanocomposites is smooth in all ranges of MWNTs concentration. The average diameter of PAA nanofibers was obtained to be 226±25 nm which increased significantly by addition of MWNTs. The diameters of PAA/MWNTs nanofibers increased to 266±40 nm, 289±47 nm, 318±43 nm, and 333±52 nm with increasing the MWNTs concentration to 0.5, 1, 2 and 3 wt %, respectively. Further increase in MWNTs concentration (i.e. 4 and 5 wt %) did not significantly influence the diameter of nanofibers (334±51 nm and 336±51 nm respectively). Increasing the average diameter of PAA/MWNTs nanofibers compared to pure PAA nanofibers could be attributed to the increasing solution viscosity with the addition of MWNTs to polymer solutions. [42]

Fig. 1

Figure 2 shows SEM image of PAA nanofibers after crosslinking and immersion in water for 24 h. Although, crosslinking and immersion in water leads to non-uniformity of the fibers surface and low shrinkage of membrane, samples retained their fibrous and 3D structure. In addition, clear swelling of nanofibers after immersion in water depicts hydrogel inherent of crosslinked PAA.

Fig. 2

3.2. Mechanical properties

Mechanical properties of PAA nanofiber layers were also investigated to confirm the crosslinking of nanofibers with GA. Figure 3 shows stress-strain curves of pure PAA nanofiber layers before and after crosslinking. As it is demonstrated, the tensile strength and modulus of nanofiber layers were increased from 0.6 ± 0.02 to 1.12 ± 0.26 MPa (1.87-fold) and 20.85 ± 1.99 to 91.54 ± 8.89 MPa (4.39-fold), after crosslinking respectively. However, the elongation at break of crosslinked sample was significantly decreased. In crosslinked nanofibers, molecular chains are tightly fettered and their sliding is difficult. Therefore, they had higher tensile strength and lower elongation at break than non-crosslinked samples. These results indicated the successful crosslinking of PAA nanofibers with GA.

Fig. 3

3.3. Thermal properties

The effect of nanofibers crosslinking and enzyme immobilization on the thermal behavior of samples was studied by TGA technique. Figure 4 shows TGA curves of pure, crosslinked and enzyme immobilized PAA nanofiber layers. PAA is a highly hydrophilic polymer and initial weight reduction in TGA curve for PAA nanofibers is due to the moisture loss. The TGA curve of PAA nanofibers shows a two-stage weight loss. Weight loss of 23% in TGA curve (near 300 ºC) of PAA nanofibers is due to dehydration of adjacent carboxylic groups to form anhydrides

which is in agreement with the work of Lu and Hsieh.[43] The majority of weight loss and decomposition in PAA nanofibers occurred near 450 ºC and about 13% of weight remained in the carbon residue. On the other hand, crosslinking of nanofibers increases thermal stability of PAA nanofibers and its curve shows a one-stage weight loss. Moreover, enzyme immobilization (immersion for 20 h at 4 ºC in enzyme solution) does not much effect the thermal stability of the nanofibers. Increasing thermal stability of PAA nanofibers is another evidence for successful cross-linking of nanofibrous membrane.

Fig. 4

3.4. FTIR spectroscopy

Figure 5 shows the FTIR spectra of PAA nanofibers before and after crosslinking. In the FTIR spectrum of PAA, the peaks around 3124, 2951 and 1708 cm^{-1} can be attributed to the stretching of O–H, C–H and C=O, respectively. The C–H stretching bands near 2951 cm^{-1} are overlapped with the O–H stretching bands. After crosslinking of PAA nanofibers, the peak at 1708 cm^{-1} related to the carboxyl group of carboxylic acid was omitted, while a new peak at 3412 cm^{-1} was observed that attributed to the formation of the silyl enol ether due to modifying with APTES and GA (Fig. 5 (b)). Also, new peak owing to carboxylate groups were appeared in the FTIR spectra of the amine-carboxylate salt absorptions at 1566 and 1353 cm^{-1}. Additionally, another peak at 1086 cm^{-1} can be attributed to Si–OEt groups of APTES. Therefore, FTIR spectroscopy confirmed the surface modification of PAA nanofibers.

Fig. 5

3.5. Assessment of immobilized AChE

AChE enzyme was immobilized on the surface of PAA nanofibers containing different concentrations of MWNTs using glutaraldehyde as a binding agent. Glutaraldehyde is a very popular crosslinker that three kinds of modifications with it can be considered in the case of enzyme immobilization: (1) the free glutaraldehyde that reacts with amino group and may react with other glutaraldehyde molecules, (2) the amino-glutaraldehyde that can react quickly with glutaraldehyde or with other amino-glutaraldehyde, and (3) the amino-glutaraldehyde-glutaraldehyde that is very reactive with amino groups even at neutral pH values.[15, 16] Under the condition of this study, it seems, the second mechanism may be occurred and the amino-glutaraldehyde reacted with other amino-glutaraldehyde.

Figure 6 shows the activity of immobilized AChE on various membranes. It is clearly observed that the activity of AChE immobilized on PAA/MWNTs nanocomposite nanofibers is considerably higher than enzyme immobilized on pure PAA membrane. The activity of immobilized AChE increases with increasing MWNTs concentration, and the immobilized enzyme on PAA/MWNTs membrane containing 4 wt% of MWNTs had the greatest activity (5.07 fold compared to pure PAA).

Generally, the improved activity of the biocatalysts using nanotubes is related to an increase of the amount of immobilized enzyme due to the high surface of nanotubes. Moreover, electrical conductivity of the membrane increases by addition of MWNTs which assists electron transfer, and hence the catalytic reaction of the enzyme will be sustainable.[38] Therefore, AChE was immobilized on PAA/MWNTs nanofibers via three mechanisms: 1) physical absorption and trapping of enzyme molecules in 3D structure of PAA nanofibers, 2) attachment of enzymes to

polymeric nanofibers using glutaraldehyde as a binding agent, and 3) physical absorption of enzymes on MWNTs surfaces.

Fig. 6

The reusability of the immobilized AChE on pure PAA and PAA/MWNTs (4 wt%) nanofibers was studied by measuring the activity after 10 reusing cycles. As observed in Figure 7, immobilized enzymes on PAA and PAA/MWNTs nanofibrous samples maintained more than 90% of their original activities after 10 cycles of washing. The small loss of activity of the immobilized enzyme may be due to enzyme desorption (of just physically adsorbed enzyme molecules) or enzyme subunit dissociation. Although, loss of enzyme activity in PAA/MWNTs sample was slightly more than pure PAA; this inconsiderable difference is due to the enzyme molecules loss from the support; the ones which are physically immobilized on nanotubes surface. This result which shows improved reusability compared to previous studies[35-37], indicates successful attachment and immobilization of AChE on PAA nanofiber membranes.

Fig. 7

PAA/MWNTs nanofibrous membrane including 4 wt% of nanotubes was chosen to compare properties of immobilized and free AChE enzymes. The kinetic parameters of free and immobilized AChE were determined using different concentrations of acetylthiocholine iodide as substrate at constant pH and temperature. Figure 8 shows Michaelis-Menten curves for free and immobilized AChE and the kinetic data are summarized in Table 1. The activity of both free and

immobilized AChE was increased with increasing ATChI concentration to a certain value and then the substrate has an inhibitory effect on the enzyme (the inhibition range has not been shown). In comparison with free AChE, K_m value for the immobilized enzyme was increased. This is attributed to the conformation changes of enzyme molecules, which impedes the enzyme-substrate interaction or it may be due to the diffusion problems. Moreover, reduction of V_{max} may be due to conformational changes of enzyme molecules or the microenvironment changes around the enzyme.[44]

Fig. 8

Table 1

The effect of medium pH on the activity of free and immobilized AChE was determined in the pH range from 5.6 to 10.2 at constant temperature (Fig. 9). As observed, the optimum pH for free and immobilized enzyme was obtained 8.5 and 8.1, respectively. A similar pH shift was also observed in other works and this change depends on ionic charge and on the nature of the support used for immobilization.[37, 45] Also, this small change in the optimum pH of free and immobilized enzyme may be due to change in enzyme structure. Moreover, in acidic pH, immobilized AChE displays higher activity than free enzyme. These results indicate that the immobilization process could enhance the pH stability of AChE at lower pH values.

Fig. 9

Figure 10 shows the effect of temperature change on the activity of free and immobilized AChE. The optimum temperature for free and immobilized enzyme was obtained at 40 ºC and 45 ºC respectively. Moreover, the immobilized enzyme retained its activity in a wider range of temperatures in comparison with free enzyme. In other words, immobilization of AChE on this type of membrane improves thermal stability of the enzyme that it may be due to multipoint interactions between enzyme and support. The multipoint immobilization of enzyme produces a more rigid structure and caused reduction of conformational changes. Therefore, the immobilized enzyme has a higher thermal stability in comparison to the free enzyme.[10, 45, 46]

Fig. 10

4. Conclusion

PAA and PAA/MWNTs nanofibrous membranes were fabricated using electrospinning method for enzyme immobilization. AChE was immobilized after modifying with APTES and GA on pure PAA nanofibers and PAA/MWNTs nanocomposite nanofibers containing different concentrations of MWNTs. The immobilized AChE on PAA nanofibers with 4 wt % of MWNTs showed the most activity compared to the other samples. The immobilized enzyme on nanofibrous samples maintained more than 90% of its original activity even after 10 cycles of reusing. In addition, the immobilization process improved pH and thermal stability of AChE. These results show that the PAA/MWNTs nanofibrous membranes are suitable candidates for immobilization of AChE and could show potential industrial applications for pesticide detection.

Acknowledgements

The authors would like to thank the Deputy of Research of Amirkabir University of Technology for funding the project. Special thanks to Shahid Beheshti University for the great help and support to do this work.

References

1. E. T. Hwang and M. B. Gu, *Eng. Life Sci.*, 2013, **13**, 49-61.
2. Z. Du, C. Li, L. Li, M. Zhang, S. Xu and T. Wang, *Mater. Sci. Eng., C*, 2009, **29**, 1794-1797.
3. F. Hasan, A. Shah and A. Hameed, *Enzyme Microb. Technol.*, 2006, **39**, 235-251.
4. M. Vellard, *Curr. Opin. Biotechnol.*, 2003, **14**, 444-450.
5. J. Kim, H. Jia and P. Wang, *Biotechnol. Adv.*, 2006, **24**, 296-308.
6. C. Chen, Q. Xie, D. Yang, H. Xiao, Y. Fu, Y. Tan and S. Yao, *RSC Adv.*, 2013, **3**, 4473-4491.
7. R. A. Sheldon and S. van Pelt, *Chem. Soc. Rev.*, 2013, **42**, 6223-6235.
8. R. DiCosimo, J. McAuliffe, A. J. Poulose and G. Bohlmann, *Chem. Soc. Rev.*, 2013, **42**, 6437-6474.
9. C. Mateo, J. M. Palomo, G. Fernandez-Lorente, J. M. Guisan and R. Fernandez-Lafuente, *Enzyme Microb. Technol.*, 2007, **40**, 1451-1463.
10. R. C. Rodrigues, C. Ortiz, Á. Berenguer-Murcia, R. Torres and R. Fernández-Lafuente, *Chem. Soc. Rev.*, 2013, **42**, 6290-6307.
11. C. Garcia-Galan, Á. Berenguer-Murcia, R. Fernandez-Lafuente and R. C. Rodrigues, *Adv. Synth. Catal.*, 2011, **353**, 2885-2904.
12. R. Fernandez-Lafuente, *Enzyme Microb. Technol.*, 2009, **45**, 405-418.
13. K. Hernandez and R. Fernandez-Lafuente, *Enzyme Microb. Technol.*, 2011, **48**, 107-122.
14. D. Brady and J. Jordaan, *Biotechnol. Lett*, 2009, **31**, 1639-1650.
15. R. C. Rodrigues, Á. Berenguer-Murcia and R. Fernandez-Lafuente, *Adv. Synth. Catal.*, 2011, **353**, 2216-2238.

16. O. Barbosa, C. Ortiz, Á. Berenguer-Murcia, R. Torres, R. C. Rodrigues and R. Fernandez-Lafuente, *RSC Adv.*, 2014, **4**, 1583-1600.

17. O. Barbosa, R. Torres, C. Ortiz, A. n. Berenguer-Murcia, R. C. Rodrigues and R. Fernandez-Lafuente, *Biomacromolecules*, 2013, **14**, 2433-2462.

18. S. A. Ansari and Q. Husain, *Biotechnol. Adv.*, 2012, **30**, 512-523.

19. Y. Masuda, S.-i. Kugimiya, Y. Kawachi and K. Kato, *RSC Adv.*, 2014, **4**, 3573-3580.

20. K. Min and Y. J. Yoo, *Biotechnol. Bioprocess Eng.*, 2014, **19**, 553-567.

21. Z. G. Wang, L. S. Wan, Z. M. Liu, X. J. Huang and Z. K. Xu, *J. Mol. Catal.*, 2009, **56**, 189-195.

22. D. Tran and K. J. Balkus, *Top. Catal.*, 2012, **55**, 1057-1069.

23. P.-C. Chen, X.-J. Huang and Z.-K. Xu, *RSC Adv.*, 2014, **4**, 6151-6158.

24. W. Feng and p. Ji, *Biotechnol. Adv.*, 2011, **29**, 889-895.

25. M. F. Yu, O. Lourie, M. J. Dyer, K. Moloni, T. F. Kelly and R. S. Ruoff, *Science,* 2000, **287**, 637-640.

26. A. Javey, J. Guo, Q. Wang, M. Lundstrom and H. J. Dai, *Nature,* 2003, **424**, 654-657.

27. S. Berber, Y.-K. Kwon and D. Tománek, *Phys. Rev. Lett.*, 2000, **84**, 4613–4616.

28. Z. Song, X. Hou, L. Zhang and S. Wu, *Materials*, 2011, **4**, 621-632.

29. M. V. Jose, B. W. Steinert, V. Thomas, D. R. Dean, M. A. Abdalla, G. Price and M. Janowski, *Polymer*, 2007, **48**, 1096-1104.

30. Z. Su, J. Ding and G. Wei, *RSC Adv.*, 2014, **4**, 52598-52610.

31. S. V. Ebadi, A. Fakhrali, A. A. Gharehaghaji, S. Mazinani and S. O. Ranaei-Siadat, *Polym. Compos.*, 2015, DOI: 10.1002/pc.23512.

32. O. Ranaei-Siadat, A. Lougarre, L. Lamouroux, C. Ladurantie and D. Fournier, *BMC. Biochem.*, 2006, **7**.

33. M. Barshan-Tashnizi, S. Ahmadian and S. O. Ranaei-Siadat, *Biotechnol. Appl. Biochem.*, 2009, **52**, 257-264.

34. A. Mutero and D. Fournier, *J. Biol. Chem.*, 1992, **267**, 1695-1700.

35. A. moradzadegan, S. O. Ranaei-Siadat, A. Ebrahim-habibi, M. Barshan-tashnizi, R. jalili, S. F. Torabi and K. Khaje, *Eng. Life Sci.*, 2010, **10**, 57-64.

36. O. Stoilova, N. Manolova, K. Gabrovska, I. Marinov, T. Godjevargova, D. Mita and I. Rashkov, *J. Bioact. Compat. Polym.*, 2010, **25**, 40-57.

37. O. Stoilova, M. Ignatova, N. Manolova, T. Godjevargova, D. G. Mita and I. Rashkov, *Eur. Polym. J.*, 2010, **46**, 1966-1974.

38. N. Amini, S. Mazinani, S. O. Ranaei-Siadat, M. R. Kalaee, S. Hormozi, K. Niknam and N. Firouzian, *Appl. Biochem. Biotechnol.*, 2013, **170**, 91-104.

39. J. W. Wang, C. Y. Chen and Y. M. Kuo, *Polym. Adv. Technol.*, 2008, **19**, 1343-1352.

40. A. Liu, I. Honma, M. Ichihara and H. Zhou, *Nanotechnology*, 2006, **17**, 2845-2849.

41. G. L. Ellman, K. D. Courteny, V. Andres jr and R. M. Featherstone, *Biochem. Pharmacol.*, 1961, **7**, 88-95.

42. K. Nasouri, A. Mousavi Shoushtari, A. Kaflou, H. Bahrambeygi and A. Rabbi, *Polym. Compos.*, 2012, **33**, 1951-1959.

43. P. Lu and Y. L. Hsieh, *Nanotechnology*, 2009, **20**, 1-9.

44. G. Bayramoglu, A. Akbulut and M. Y. Arica, *J. Hazard. Mater.*, 2013, **244**, 528-536.

45. H. Tümtürk, F. Şahin and G. Demirel, *Biotechnol. Bioproc. E.*, 2007, **30**, 141-145.

46. U. Guzik, K. Hupert-Kocurek and D. Wojcieszyńska, *Molecules*, 2014, **19**, 8995-9018.

Table 1. Kinetic parameters of free and immobilized AChE.

Enzyme	K_m (mM)	V_{max} (μmol/min)
Free AChE	0.0552	0.0518
Immobilized AChE	0.1241	0.0441

Figure Captions:

Figure 1. SEM images of PAA/MWNTs nanocomposite nanofibers with different amount of MWNTs. (a) 0 wt%, (b) 0.5 wt%, (c) 1 wt%, (d) 2 wt%, (e) 3 wt%, (f) 4 wt% and (g) 5 wt% of MWNTs.

Figure 2. SEM image of crosslinked PAA nanofibers.

Figure 3. Stress-strain curves for PAA nanofiber layers before and after crosslinking.

Figure 4. TGA curves of PAA nanofibers before and after crosslinking and enzyme immobilization.

Figure 5. FTIR spectra of PAA nanofibers before and after crosslinking.

Figure 6. Activity of immobilized AChE on pure PAA and different PAA/MWNTs nanofibers. Error bars represent mean ± standard deviation (n=3).

Figure 7. Reusability of immobilized AChE on pure PAA and PAA/MWNTs nanofibers.

Figure 8. Michaelis– Menten curves of free and immobilized AChE.

Figure 9. Effect of pH on the activity of free and immobilized AChE.

Figure 10. Effect of temperature on the activity of free and immobilized AChE.

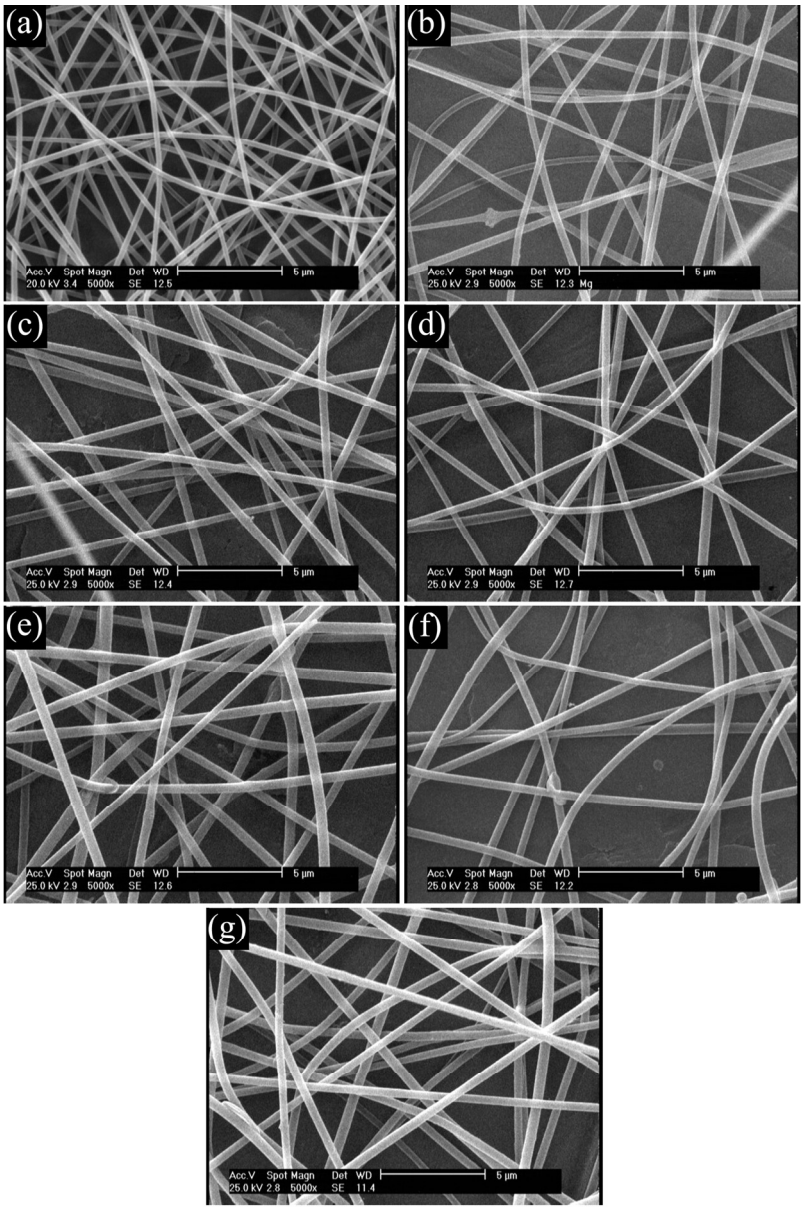

Figure 1. SEM images of PAA/MWNTs nanocomposite nanofibers with different amount of MWNTs. (a) 0 wt%, (b) 0.5 wt%, (c) 1 wt%, (d) 2 wt%, (e) 3 wt%, (f) 4 wt% and (g) 5 wt% of MWNTs.
129x195mm (300 x 300 DPI)

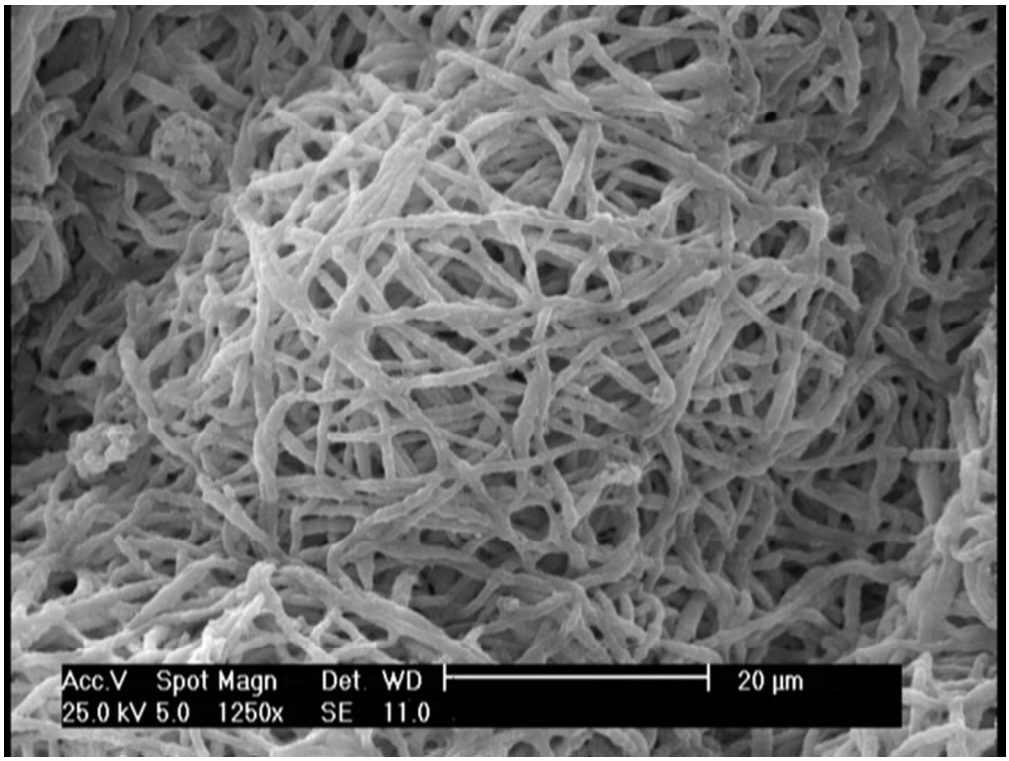

Figure 2. SEM image of crosslinked PAA nanofibers.
82x61mm (300 x 300 DPI)

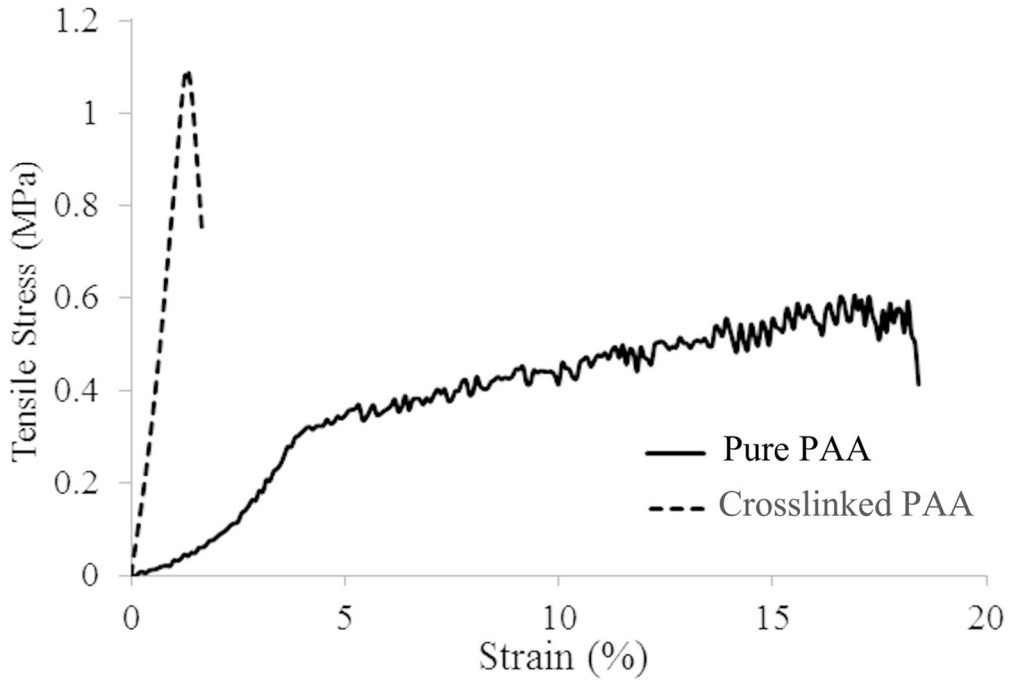

Figure 3. Stress-strain curves for PAA nanofiber layers before and after crosslinking.
60x43mm (600 x 600 DPI)

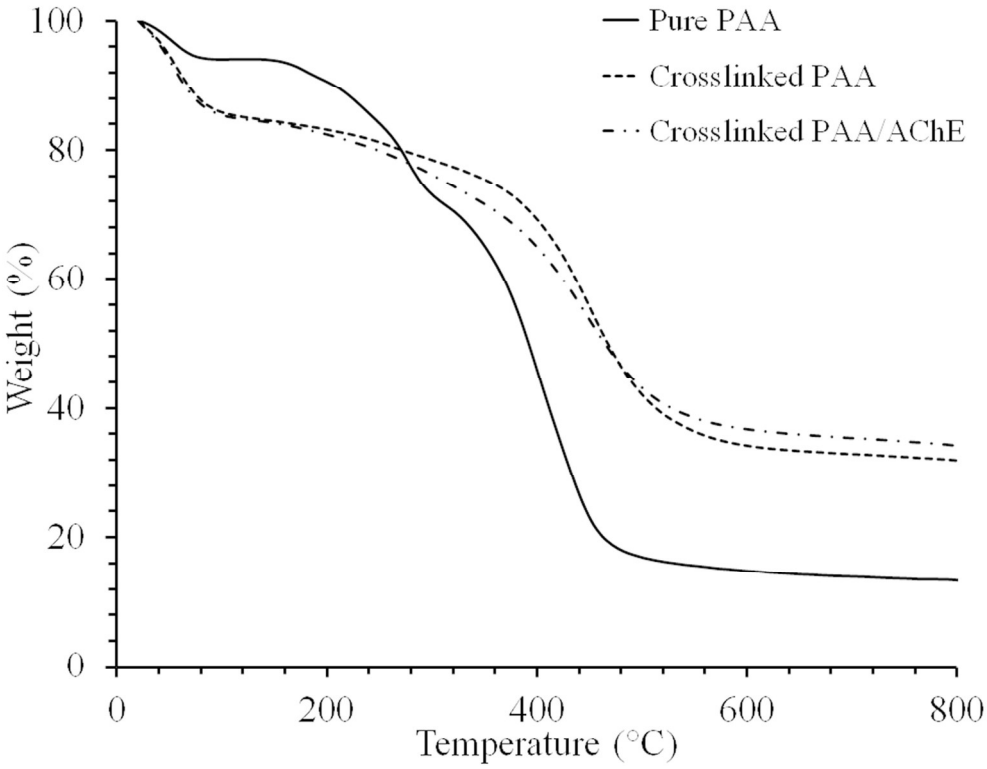

Figure 4. TGA curves of PAA nanofibers before and after crosslinking and enzyme immobilization.
63x49mm (600 x 600 DPI)

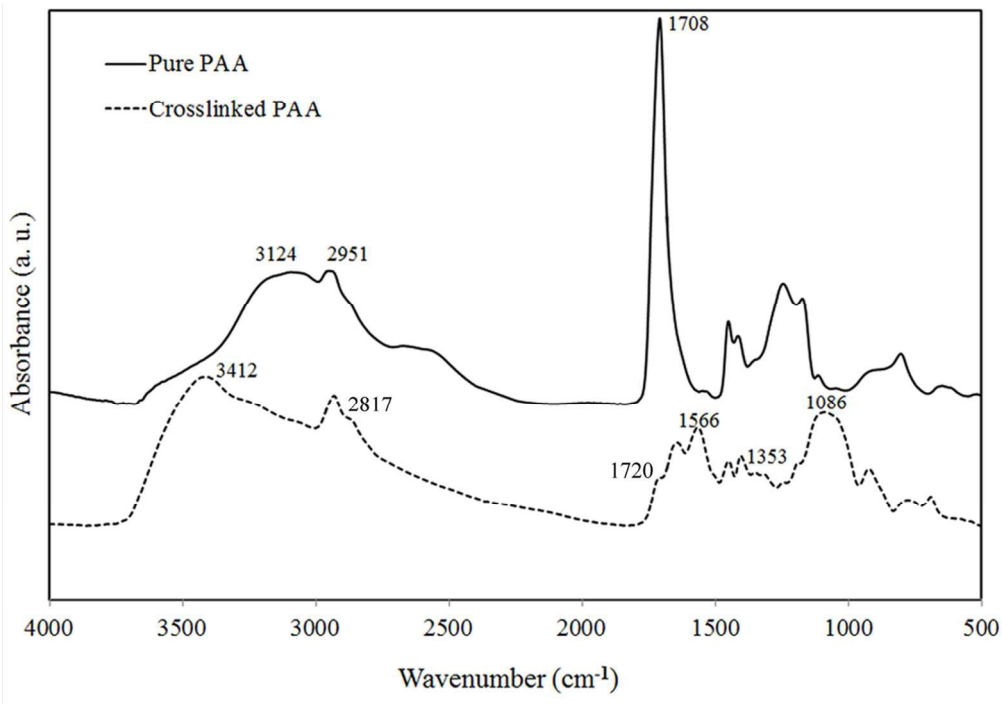

Figure 5. FTIR spectra of PAA nanofibers before and after crosslinking.
57x40mm (600 x 600 DPI)

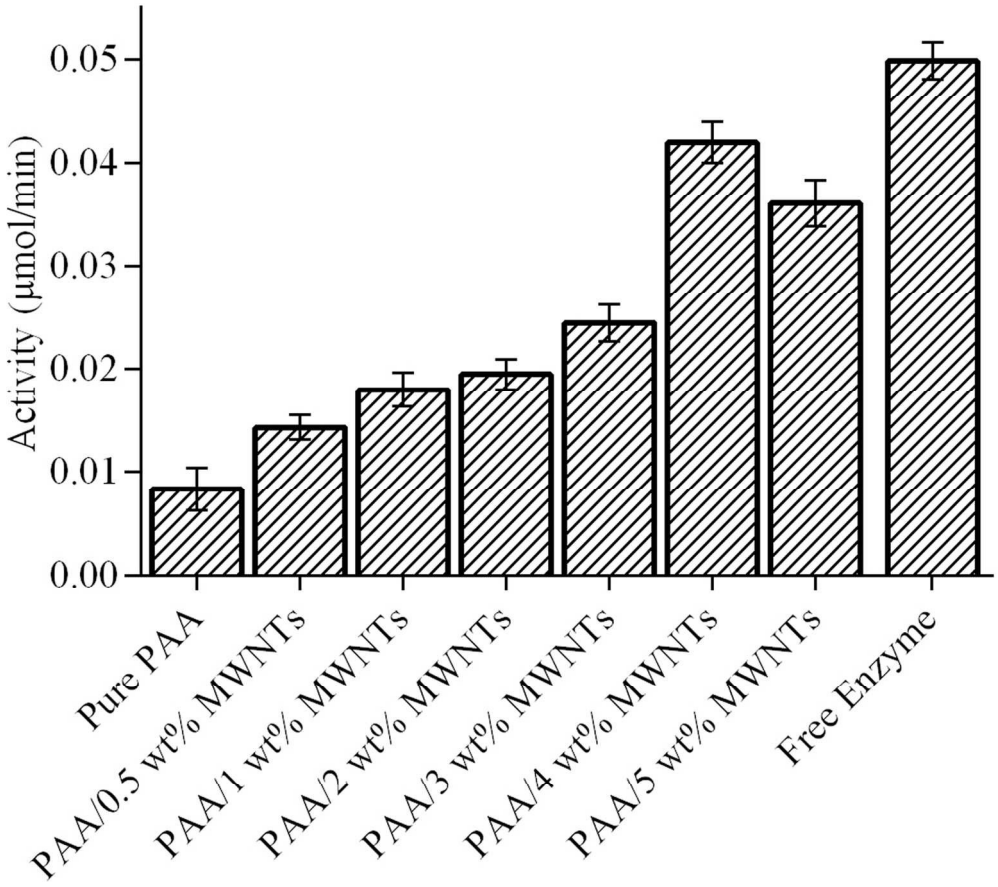

Figure 6. Activity of immobilized AChE on pure PAA and different PAA/MWNTs nanofibers. Error bars represent mean ± standard deviation (n=3).
72x64mm (600 x 600 DPI)

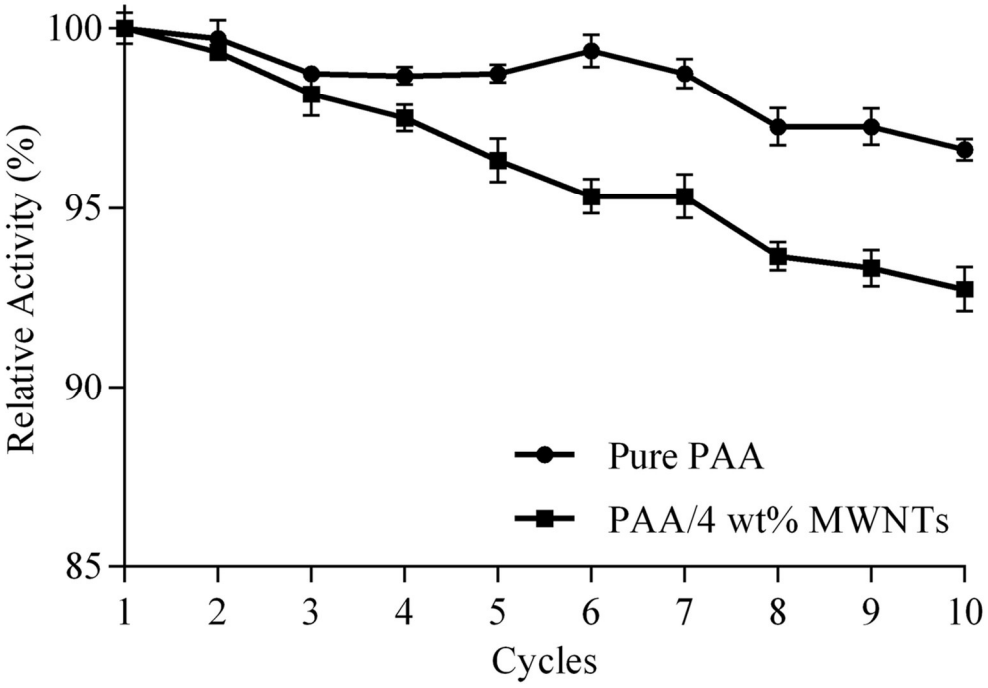

Figure 7. Reusability of immobilized AChE on pure PAA and PAA/MWNTs nanofibers.
57x39mm (600 x 600 DPI)

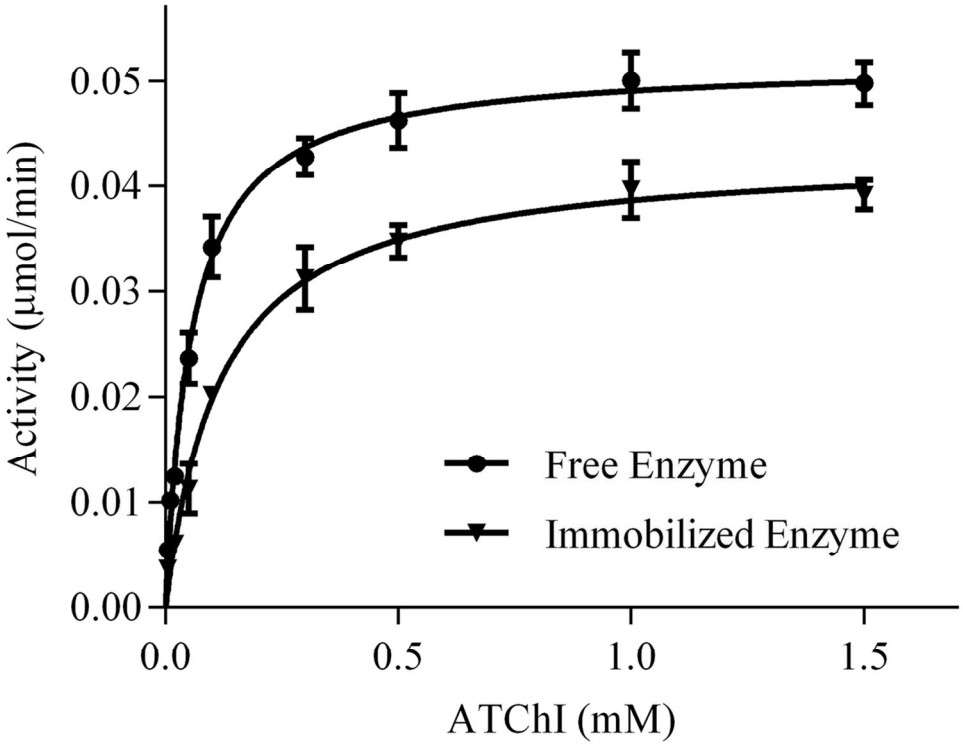

Figure 8. Michaelis– Menten curves of free and immobilized AChE.
63x48mm (600 x 600 DPI)

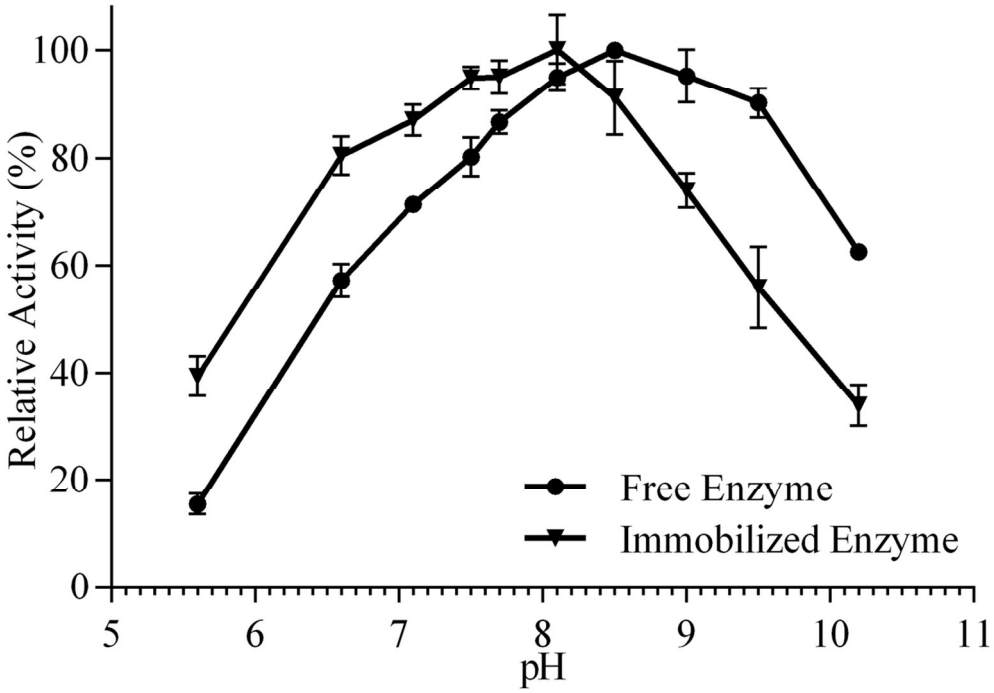

Figure 9. Effect of pH on the activity of free and immobilized AChE.
57x40mm (600 x 600 DPI)

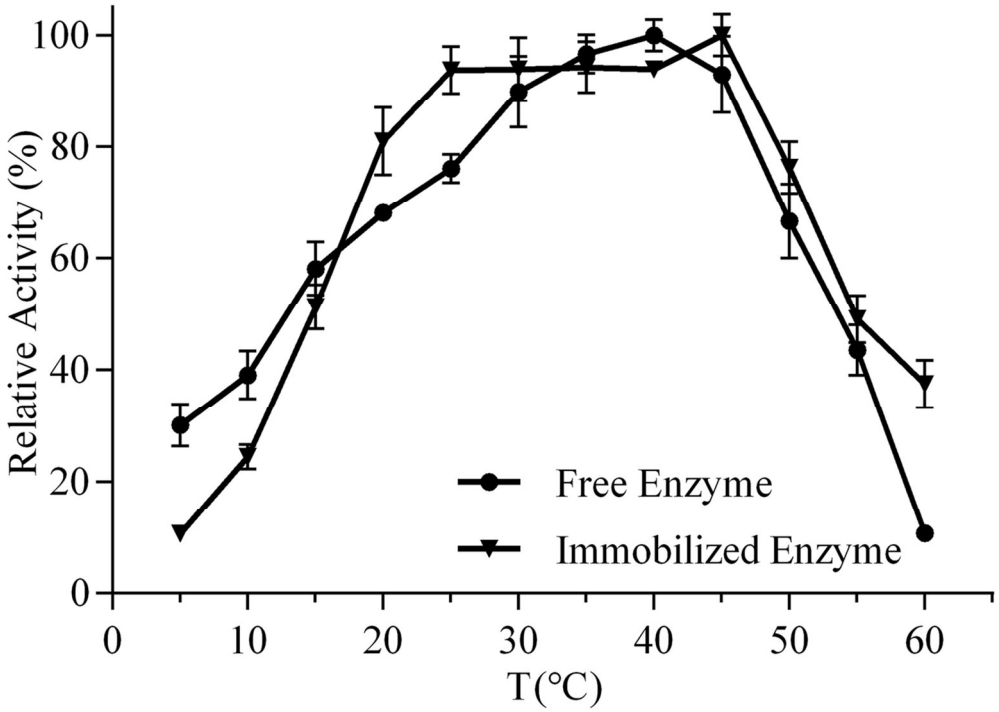

Figure 10. Effect of temperature on the activity of free and immobilized AChE.
58x41mm (600 x 600 DPI)

The immobilized enzyme on nanofibrous samples maintained more than 90% of its original activity even after 10 cycles of reusing.

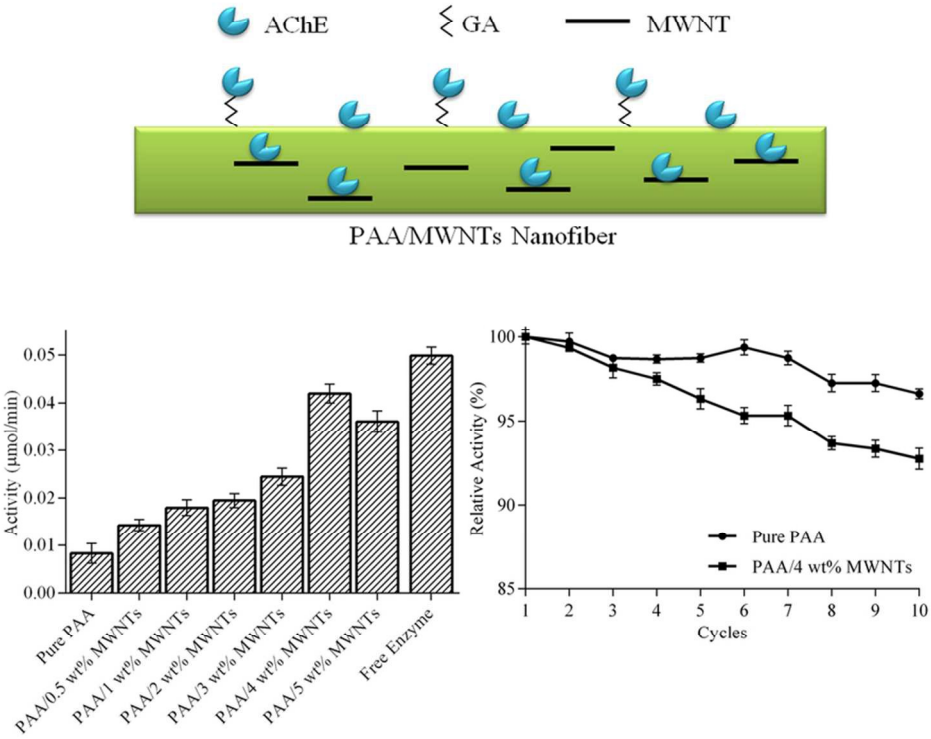

table of contents
40x32mm (600 x 600 DPI)